



University of HUDDERSFIELD

University of Huddersfield Repository

MacEwen, Howard A., Fazio, Giovanni G., Lystrup, Makenzie, Batalha, Natalie, Siegler, Nicholas, Tong, Edward C., Veenendaal, Ian, Naylor, David, Gom, Brad, Gunuganti, Sudhakar, Winter, Calvin, Jones, Martyn and Walker, David D.

Performance of a cryogenic test facility for 4 K interferometer delay line investigations

Original Citation

MacEwen, Howard A., Fazio, Giovanni G., Lystrup, Makenzie, Batalha, Natalie, Siegler, Nicholas, Tong, Edward C., Veenendaal, Ian, Naylor, David, Gom, Brad, Gunuganti, Sudhakar, Winter, Calvin, Jones, Martyn and Walker, David D. (2016) Performance of a cryogenic test facility for 4 K interferometer delay line investigations. In: *Space Telescopes and Instrumentation 2016*, June 26 2016, Edinburgh.

This version is available at <http://eprints.hud.ac.uk/30379/>

The University Repository is a digital collection of the research output of the University, available on Open Access. Copyright and Moral Rights for the items on this site are retained by the individual author and/or other copyright owners. Users may access full items free of charge; copies of full text items generally can be reproduced, displayed or performed and given to third parties in any format or medium for personal research or study, educational or not-for-profit purposes without prior permission or charge, provided:

- The authors, title and full bibliographic details is credited in any copy;
- A hyperlink and/or URL is included for the original metadata page; and
- The content is not changed in any way.

For more information, including our policy and submission procedure, please contact the Repository Team at: E.mailbox@hud.ac.uk.

<http://eprints.hud.ac.uk/>

Performance of a cryogenic test facility for 4 K interferometer delay line investigations

Ian Veenendaal^{*a}, David Naylor^a, Brad Gom^a, Sudhakar Gunuganti^{a,b}, Calvin Winter^c, Martyn Jones^d, David Walker^d

^aAstronomical Instrumentation Group, Department of Physics and Astronomy, University of Lethbridge, 4401 University Drive W., Lethbridge, Alberta, Canada T1K 3M4;

^bBlue Sky Spectroscopy, Suite 9 - 740 4th Avenue South, Lethbridge AB Canada T1J 0N9;

^cQuantum Technology Corp – CANADA, 3200 University Blvd., Squamish, BC V8B 0N8, Canada;

^dGlyndŵr University, Mold Road, Wrexham LL11 2AW, United Kingdom

ABSTRACT

The next generation of space-borne instruments for far infrared astronomical spectroscopy will utilize large diameter, cryogenically cooled telescopes in order to achieve unprecedented sensitivities. Low background, ground-based cryogenic facilities are required for the cryogenic testing of materials, components and subsystems. The University of Lethbridge Test Facility Cryostat (TFC) is a large volume, closed cycle, 4 K cryogenic facility, developed for this purpose. This paper discusses the design and performance of the facility and associated metrology instrumentation, both internal and external to the TFC. Additionally, an apparatus for measuring the thermal and mechanical properties of carbon-fiber-reinforced polymers is presented.

Keywords: Cryogenics, cryostat design, far infrared astronomy, material characterization, Carbon-fiber-reinforced polymer

1. INTRODUCTION

The European Space Agency's Herschel Space Observatory¹ represented a major step forward in terms of both the sensitivity and spatial resolution of far infrared spectroscopic measurements of astronomical sources. Whereas Herschel's suite of instruments were cooled to temperatures of ~4 K, its primary mirror could only be passively cooled to an operational temperature of ~85 K¹. The relatively large thermal background from the Herschel telescope limited the sensitivity of the broadband spectrometers. The next generation of far infrared space borne observatories will feature large aperture actively cooled telescopes (<6 K²) to essentially eliminate this thermal background, resulting in gains of over two orders of magnitude in sensitivity compared with Herschel³. As new instrument concepts are developed to exploit the low background environment of actively cooled telescopes, there is a need for ground based cryogenic facilities with sufficient volume and cooling power to test materials and components for far infrared spectroscopic instrumentation at equivalent background levels. To this end a large-scale, cryogen-free test facility cryostat has been developed by the Astronomical Instrumentation Group (AIG) at the University of Lethbridge, in collaboration with Quantum Technology Corporation. We outline the design considerations and performance specifications of the newly built Test Facility Cryostat (TFC), and describe the complementary suite of diagnostic instrumentation.

While the ultimate purpose of the TFC is to test complete, self-contained spectrometers, along with an internal source and detector, the facility also serves as a general purpose cryogenic facility for testing material properties at low temperatures. As an example of the latter, we discuss in this paper the measurement of the temperature-dependent thermal expansion of carbon fiber reinforced polymers (CFRPs) in the 300 to 4 K range. This project formed part of a study of CFRP optical components manufactured by Glyndwr University as part of the FP7-FISICA program⁴.

2. CRYOSTAT DESIGN

Several designs were considered for the TFC, including a horizontal, cylindrical vessel⁵. The purpose of the horizontal design was to maximize the usable 4 K volume inside a simple cylindrical vacuum chamber. Figure 1 shows the cantilevered mechanical support structure of the original design. Simulations showed, however, that this structure could not be made stiff enough to reduce vibrational mode amplitudes to levels required for sensitive interferometric measurements (Figure 1). After several design iterations, a rectangular, vertical design was selected. The rectangular

arrangement provided better mechanical stiffness as well as ease of access, both in terms of the cryogenic work space and optical access via multiple viewports on the external vacuum vessel (Figure 2). The design included careful study of all heat transfer mechanisms within the TFC. Details of the design are given in the following sections.

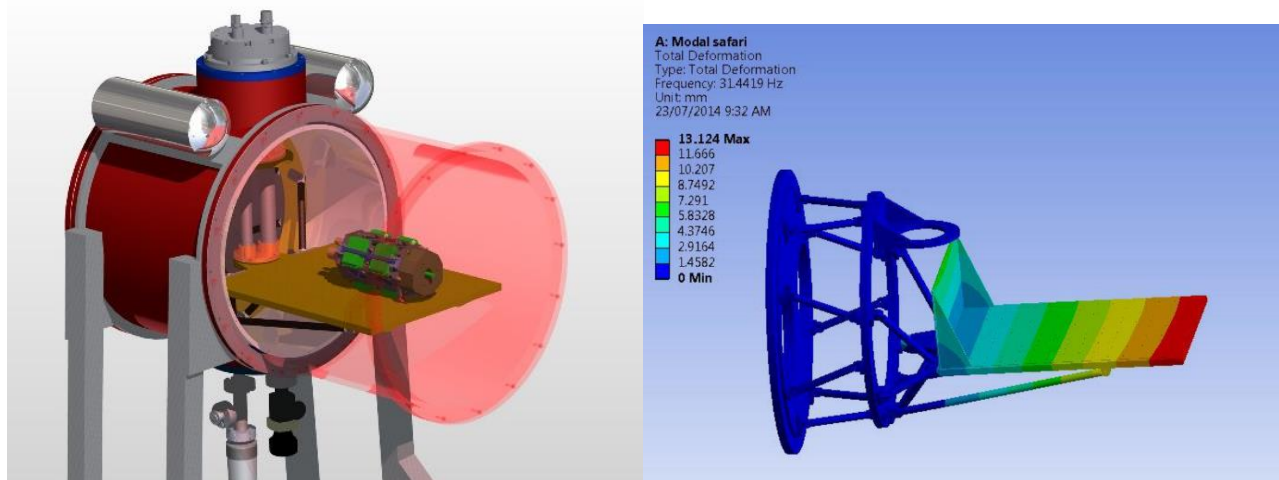


Figure 1. Renderings of the original design for the Test Facility Cryostat. (Left) The outer vacuum chamber is shown in red. The transparent section of the chamber is removable to access the 4 K volume. (Right) An FEA simulation of the first vibrational mode for the original TFC design (scale is arbitrary). The large amplitude oscillations near the end of the cantilevered plate made this design unsuitable for sensitive interferometric measurements.

2.1 Vacuum Chamber

The main body of the outer vacuum chamber (OVC) is constructed from welded 9.5 mm thick AISI type 304 stainless steel plate, selected for its high yield strength and weldability. The top plate, however, is 20 mm thick 6061-T6 aluminum alloy, chosen for its relatively easy machinability, and also because the top plate must necessarily be thicker to allow for internal threaded blind holes to attach the internal support structures. The vacuum chamber is split horizontally across the middle and a scissor lift is incorporated into the cryostat support frame to allow the heavy OVC to be raised and lowered with ease. This provides convenient access to either the lower 4 K working volume, or the upper wiring harness and support framework, by lowering either the bottom half of the OVC, or the entire OVC, respectively.

The 4 K working volume of the TFC is surrounded with removable flanges, which provide a means of coupling external optics to instrumentation in the internal cryogenic chamber. The rectangular design allows access to any part of the 4 K volume from at least one of the nine available ports. One 150 mm diameter port and two 70 mm diameter ports are situated on each long side of the OVC, one 70 mm port on each of the short sides, and one 70 mm port on the underside. These flanges also provide the option of adding mechanical feedthroughs for mechanical property measurements of cooled samples.

2.2 Cooling Mechanism

The TFC was designed to accommodate two identical Cryomech PT415 pulse tube coolers⁶ (PTCs). While the system can operate with only a single PTC, the additional cooling power of the second PTC improves the cooldown time and cooling power at the base temperature. Mechanical cryocoolers offer several advantages over conventional liquid helium cryostats, including the inconvenience, expense, and potential hazards associated with handling liquid cryogens. Each PTC provides 1.5 W of cooling power at 4.2 K, and an additional 40 W of cooling power at an intermediate stage at 45 K⁶. The main disadvantage of PTCs is that they introduce vibrations into the cryostat from oscillating helium gas within the cooler. To minimize the impact of these vibrations, the cold heads at both stages of the PTC are attached to the cryostat cold stages with flexible oxygen-free, high-conductivity (OFHC) copper braids which provide a good thermal conduction path while decoupling mechanical vibrations (Figure 3). The braids have a length of 110 mm and a total cross-sectional area of 128 mm². The cold plates themselves were manufactured from 12.7 mm thick OFHC copper and both the plates and braids

were gold plated with pure 24K gold plating solution to a nominal thickness of 5 μm for better thermal conductivity at mechanical connections and reduced emissivity.



Figure 2. (Left) The TFC after delivery to the University of Lethbridge. A single PTC can be seen on the top plate. The horizontal split in the vacuum chamber allows for the bottom half of the chamber to be lowered by the scissor jack. Three blank flanges for the side apertures are also shown. (Right) A cross sectional view of the TFC. The dual pulse tube arrangement, CFRP supports, and rectangular, paneled shields are shown.

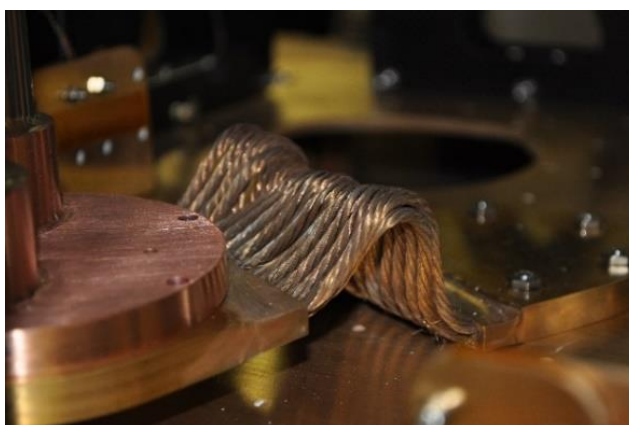


Figure 3. An image of the OFHC copper braid, with a 5 μm gold coating, connecting the 4 K pulse tube cold head and the 4 K plate. The flexible copper braids decouple the system from mechanical vibrations generated by the pulse tube, while maintaining high thermal conductivity.

2.3 Mechanical Supports

The cold heads can support a maximum load of 10 kg and 5 kg for the first and second stages respectively⁶, but the total mass of cold plates and radiation shields is approximately 20 kg for the first stage and 40 kg for the second stage. To accommodate the mass of the shields and cold plates, as well as the added mass of the systems under test, a series of CFRP plates provide mechanical coupling between the interior cold surfaces and the OVC top plate (Figure 4). CFRP was selected for its high stiffness, low thermal conductivity, and low coefficient of thermal expansion (Figure 5). This allowed the construction of thin supports which conduct minimal heat, especially at low temperatures. The rigidity of the CFRP supports helps ensure that the optical axis of an instrument mounted on the 4 K stage does not shift significantly with respect to the OVC due to mechanical vibrations, and that shifts due to thermal contraction during cooldown are minimized. The supports were machined from commercially available CFRP sheets to reduce thermal conduction cross section while retaining rigidity, using waterjet cutting to minimize fraying of the sheets at the edges. The CFRP supports were installed in a parallel sheet configuration for added rigidity, as well as ease of removal and access to the internal volume when necessary. Bolt holes in the CFRP supports were slotted to accommodate differential thermal contraction of the copper cold plates relative to the CFRP sheets, and also to relax machining tolerances of the assembly.

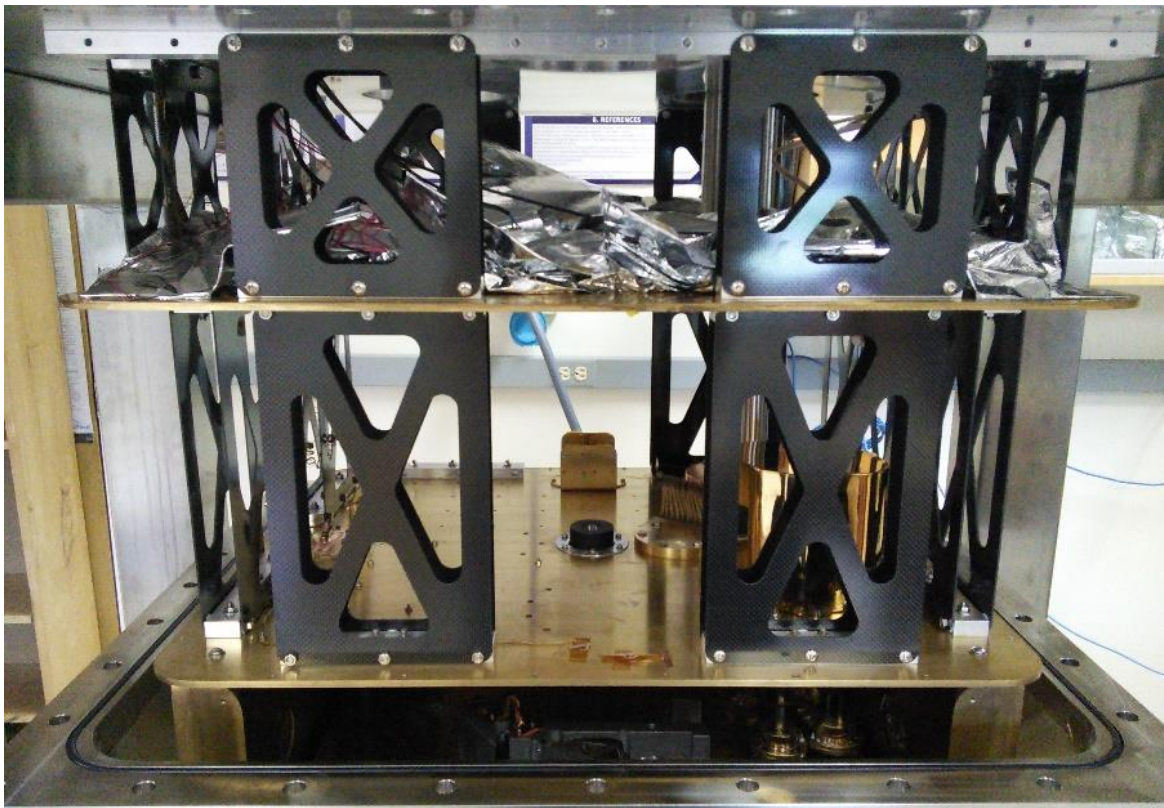


Figure 4. The upper levels of the TFC, showing the CFRP support plates. The top of the image shows the underside of the room temperature aluminum plate. The 45 K plate is pictured in the center of the image and the 4 K plate near the bottom. Below the extent of the photograph are the 4 K shields and the 4 K optical bench enclosed within.

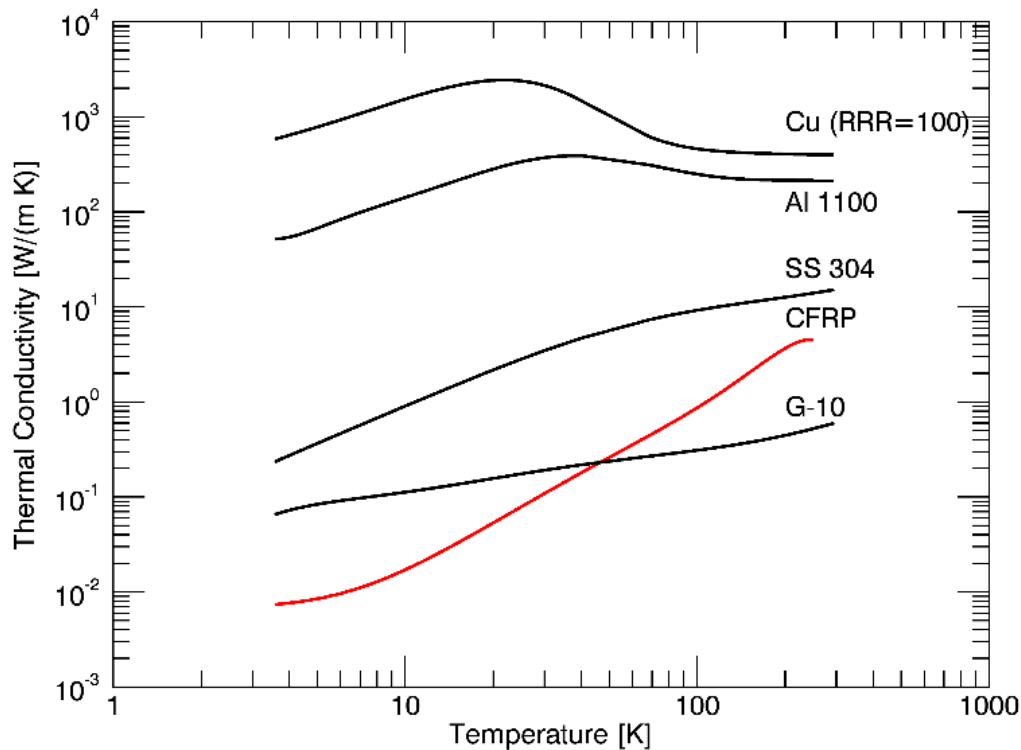


Figure 5. The thermal conductivity of CFRP rods, shown in red, from room temperature to 4 K. The thermal conductivities of other common cryostat materials are shown as a comparison. The CFRP data are measured values; data for the other materials are taken from the NIST cryogenic material properties database⁷.

2.4 Radiation Shielding

Two radiation shields surround the 4 K volume, connected to the 45 K and 4 K PTC stages respectively. The warmer first stage shield is aluminum wrapped in loose fitting aluminized Mylar multi-layer insulation (MLI); individual sheets being $\sim 20 \mu\text{m}$ thick. The MLI was cut to size for each of the 45 K plate panels and was attached and sealed at the edges. Holes were punctured into the edges of the MLI enabling the panels to be fastened together. Small perforations were also made to expedite outgassing between the layers. All panels of the 45 K shield and the top of the 45 K plate are covered in 20 layers of MLI, which proved to be sufficient for the shields to reach a temperature of less than 100 K (Section 3.2). The second stage shields are constructed from OFHC copper, and gold plated to $\sim 1 \mu\text{m}$ thickness to decrease the emissivity of the shield surface. The 4 K radiation shields reach a temperature of 9 K at the warmest point and enclose the 4 K optical bench.

2.5 Electrical Wiring

Since the TFC is a general purpose facility for testing cryogenic instruments, a range of electrical connections are required for actuators and transducers. A key consideration in the wiring harness is the wire type, diameter and length which must be carefully selected for each application to minimize heat flow, while also meeting current carrying capacity requirements. The selection of appropriate wire parameters was determined by striking a balance between minimizing heat conduction down the wires from room temperature and minimizing Joule heating generated by current flowing in the wires. The Joule heating is given by $P = I^2 R$; the thermal heat conduction is calculated using an integral form of Fourier's Law,

$$\dot{q}_{cond} = \frac{A}{L} \int_{T_1}^{T_2} \lambda(T) dT. \quad (1)$$

The wiring is divided into two groups: low current transducer wiring, and high current actuator wiring. Thermometry wiring consisted of looms of 12 twisted pairs of 90 μm diameter copper wiring. Although copper is usually avoided for low current wiring as the heat conduction is much higher than other material options, the extremely thin wire mitigated this issue. In addition, each Detronics DT series⁸ 23-pin hermetic connector on the room temperature connector flange of the TFC is associated with five CernoxTM resistance temperature detectors (RTDs). With a four-wire measurement for each of the ten thermometers connected in this way, three wires are spare in each loom. Using copper allows for some spare wires on the loom to be used to connect small heating elements if necessary. Where wire looms could not be used for thermometers, 127 μm diameter, quad-twist, phosphor bronze wiring is used⁹. This allows multiple thermometers connected to a single electrical socket to be located on different cold stages of the cryostat. Five thermometers are connected in this way, measuring the temperatures of components above the 4 K volume. In total, 20 phosphor-bronze wires and 40 copper wires are used for 15 thermometers within the cryostat. 6 copper wires are left available as spares. Approximately one meter of wire is used between the room temperature and 45 K stages and another 1 meter between the 45 K and 4 K stages.

One 23-pin electrical socket on the TFC is dedicated for high current applications (up to 500 mA). This socket is currently wired to a room temperature diode laser for optical metrology. In this case, wire selection is not critical since thermal loading is not a concern. However, there are high current wires reaching the 4 K stage for driving the scanning arm of a far infrared interferometer and operating a stepper motor controlled iris. For these applications, 34 AWG copper, twisted pair wires are used.

Table 1. Provisional wiring for TFC. The number and diameter of high current wiring is subject to change, depending on the current use of the TFC.

Number of wires	Material	Diameter (μm)
46	Copper	90
20	Phosphor Bronze	127
22	Copper	160

2.6 External Instrumentation

The TFC is equipped with multiple viewports, to which external instruments may be coupled in order to facilitate high precision measurements at 4 K. The instruments that are used are those for which there is no feasible low temperature counterpart that may be placed inside the cryostat. Currently two external instruments find extensive use: a Renishaw differential interferometer¹⁰, and a PLX autocollimator¹¹.

The Renishaw Differential Interferometer uses a HeNe laser coupled by an optical fiber to a head which mounts on the exterior of the TFC vacuum chamber (Figure 6). The head consists of optical components for a double-pass, differential interferometer and a detector. With fringe counting capabilities, this instrument measures the relative displacement of a plane mirror target with respect to a reference mirror with a resolution of 38.6 pm.

The PLX autocollimator, shown in Figure 7, is an electronically controlled instrument which measures the tilt of a plane mirror target. With an 84° x 84° field of view, the autocollimator can measure the tilt of a plane mirror up to 42' with a precision of 2.5'' and a resolution of 0.1''. In addition, this system has been used to test for performance degradation of corner cube retroreflectors from a cryogenic cooling cycle.

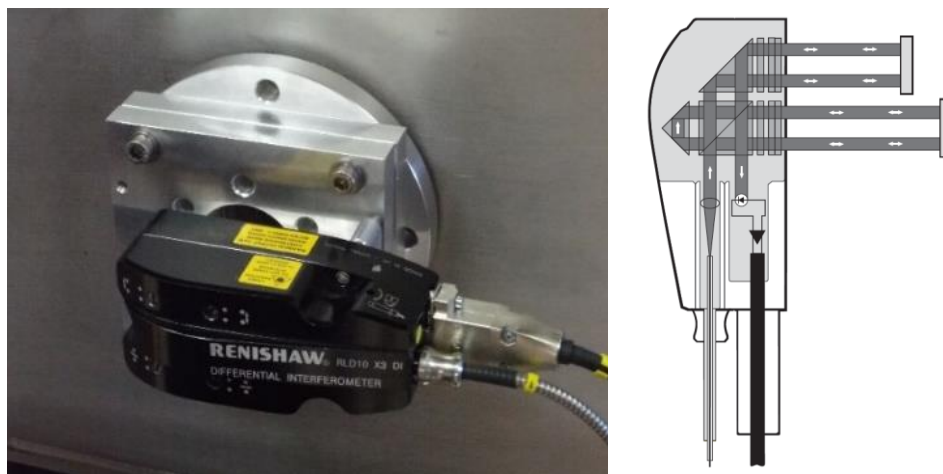


Figure 6. (Left) An image of the Renishaw RLD10 differential interferometer, mounted to the TFC with a custom-made set of aluminum plates. The plates allow for slight positional corrections to be made outside the cryostat, as well as easy detachment and re-attachment of the interferometer without realignment. (Right) A schematic, showing the optical layout of the interior of the RLD10 differential interferometer¹⁰.

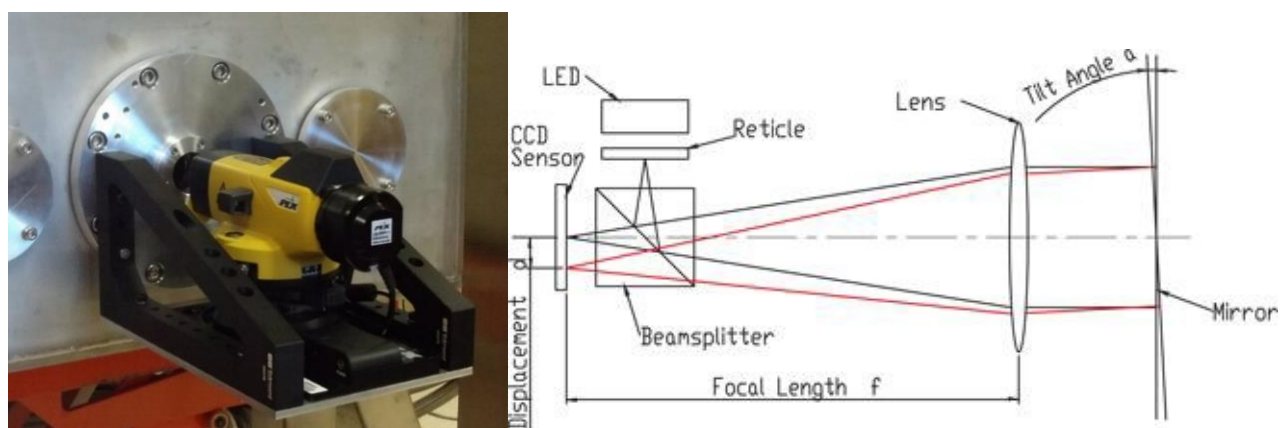


Figure 7. (Left) An image of the PLX electronic autocollimator mounted on one of the large viewports in the TFC. A shelf was constructed to hang from the viewport so that the autocollimator could be mechanically coupled to the TFC to reduced vibrational errors in the measurements. The viewport flange, shelf, and autocollimator can be removed from the TFC as a single unit. (Right) A schematic, showing the operation of the autocollimator¹¹.

3. TFC PERFORMANCE

The performance of the TFC has been evaluated over several cooldown cycles. The TFC reaches a base temperature of 3.5 K with a single pulse tube cooler in approximately 25 hours. In this section, we discuss the cooling specifications, both predicted and measured and the cooling power at base temperatures.

3.1 Vacuum

The TFC is evacuated using a 4-foot-long, KF40 bellows, and an Edwards XDS35i dry scroll vacuum pump¹². The roughing pump allows for a base pressure of 1 mTorr to be reached in around 15-20 hours. However, since the cool down takes a substantial amount of time, it is usually safe to begin the cooling cycle once the pressure reaches around 10 mTorr, which occurs after about 4 hours. The residual pressure is measured with an MKS 910 DualTrans Vacuum Transducer¹³. While turbo pumps are required for cryogenic facilities operating at liquid nitrogen temperatures, a roughing pump is

sufficient for the TFC operation. Once the temperature of the second stage of the PTC drops below 77 K, cryopumping of residual atmospheric gases occurs and the pressure abruptly drops to 10^{-5} Torr, the limit of the gauge.

3.2 Cooling Time

The TFC was designed to cool down in around 24 hours with one PTC. In practice the system takes approximately 25 hours to reach 4 K, although the cooling time may vary depending on the heat capacity of the experimental setup. Figure 8 shows a typical cool down curves for various elements of the TFC. The base temperature of the cold plate attached to the 4 K cold head is 3.5 K, while the base temperature of the 45 K stage is 60 K. The disparity between the 45 K cold head and 45 K stage temperatures is a result of insufficient thermal conduction through the flexible braid links. A new braid system is being developed which will allow for the 45 K stage to reach even lower temperatures (Section 5.3).

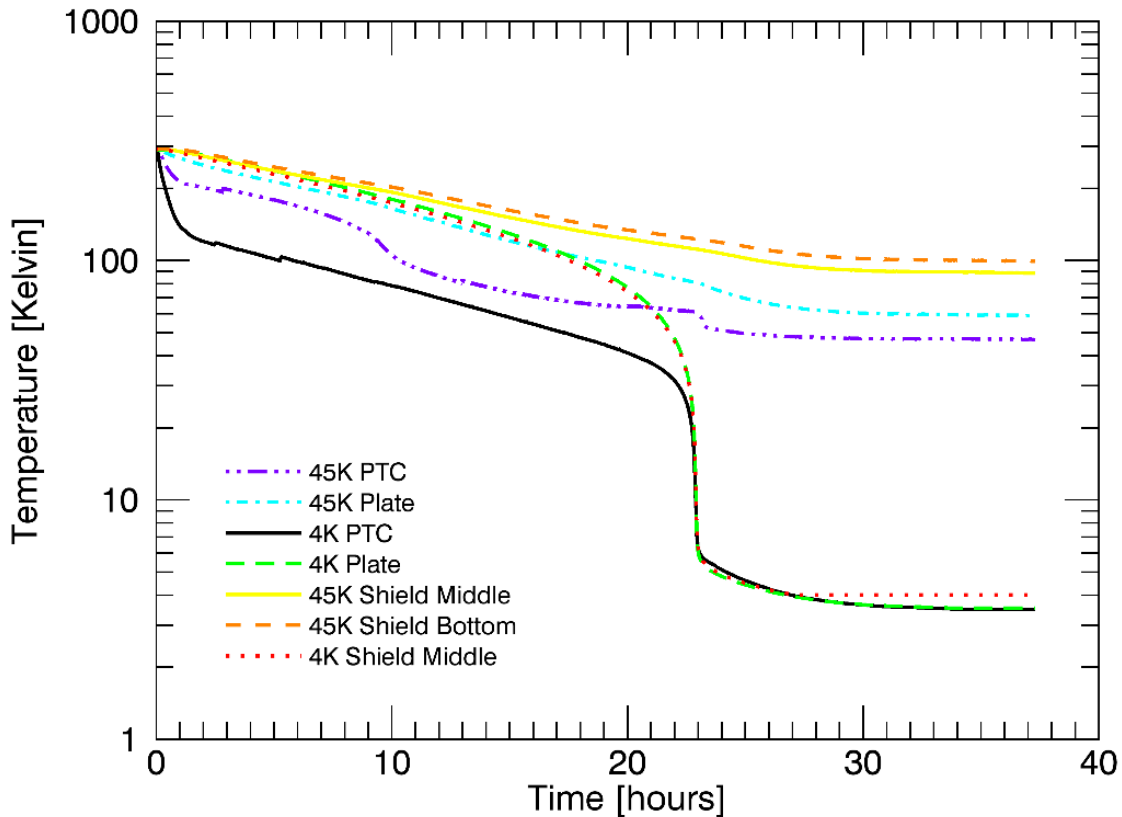


Figure 8. A plot of the PTC cold head, plate, and shield temperatures during a typical cool down of the TFC.

3.3 Cooling Power

To measure the residual cooling power at base temperatures on the 4 K bench, a large 5 W heater was placed on one end of the 4 K bench. Two thermometers, one placed near the heater and one on the furthest edge of the plate, measured the thermal gradient across the plate during these tests. The heater was wired to a PID control system internal to a Lakeshore 340 temperature controller. As the temperature was adjusted to different set points, the current through the heater was controlled and the voltage drop across the heater was measured using separate measurement leads. The heater output power ($P=VI$) was recorded as the residual cooling power at the temperature of the plate once the temperature of the plate reached equilibrium. From the results, we conclude that 1.25 W of the 1.5 W cooling power available from a single PTC is lost to parasitic heating effects of the supports, wires, and shields, leaving 250 mW of cooling power available at 4 K.

Table 2. Performance specifications of the TFC.

Parameter	Predicted (with 2 PTCs)	Actual (with 1 PTC)
Size	1.5m x 0.75 m x 2 m	1.5m x 0.75 m x 2 m
4 K Volume	580 mm x 480 mm x 250 mm	580 mm x 480 mm x 250 mm
MLI	Up to 30 layers	20 layers
Pump Out Time	< 8 hours	4 hours to 10 mTorr
Cool Down Time	< 24 hours	25 hours
Warm Up Time	24 hours	40 hours
Cooling Capacity	1.5 W	250 mW
Thermometry Channels	Up to 16	15
Viewports	2 x 150 mm dia., > 2 x 70 mm dia.	2 x 150 mm dia., 7 x 70 mm dia.

4. CFRP THERMAL TESTING RESULTS

One of the first tests of the TFC was to measure the thermal expansion of CFRP. CFRPs are a class of composite material consisting of two components: a polymer resin matrix, and carbon fibers. CFRPs exhibit favorable properties for structural components, such as high stiffness, tensile strength, and a high strength-to-mass ratio. Additionally, CFRPs can be designed to have a very low thermal expansion, as well as a low thermal conductivity. These mechanical and thermal properties make CFRP a strong contender for mechanical supports in cryogenic applications. A disadvantage of CFRP, however, is that the thermal properties of the material depend strongly on the type, density, orientation, and size of fibers used, as well as the type of polymer resin. Therefore, it becomes necessary to measure the thermal properties of each CFRP composition and fabrication process. In the following section, we outline an apparatus that was designed to measure the thermal expansion of CFRP plates from 4 to 300 K. The measurement of CFRP thermal properties was done in collaboration with Glyndwr University, under the EU FP7-FISICA program. The goal of this study was to determine the feasibility of using CFRP in the design of lightweight, cryogenic mirrors for space interferometry⁴.

4.1 Apparatus

The measurement of the thermal contraction of CFRP was performed using the Renishaw Differential Interferometer. This instrument measures the relative displacement between two mirrors, so the apparatus was designed as a straight-legged tripod configuration of CFRP plates attached to aluminum plates on either end (Figure 9). These plates held the mirror targets, and the interferometer measurement beams were directed along the axis of the CFRP samples. By recording the relative displacement over an entire cooling cycle, the total thermal contraction could be determined for any temperature range between 4 K and 300 K. Thermometers were attached to both end plates and across the CFRP to determine the temperature of each mirror and any thermal gradients present across the CFRP.

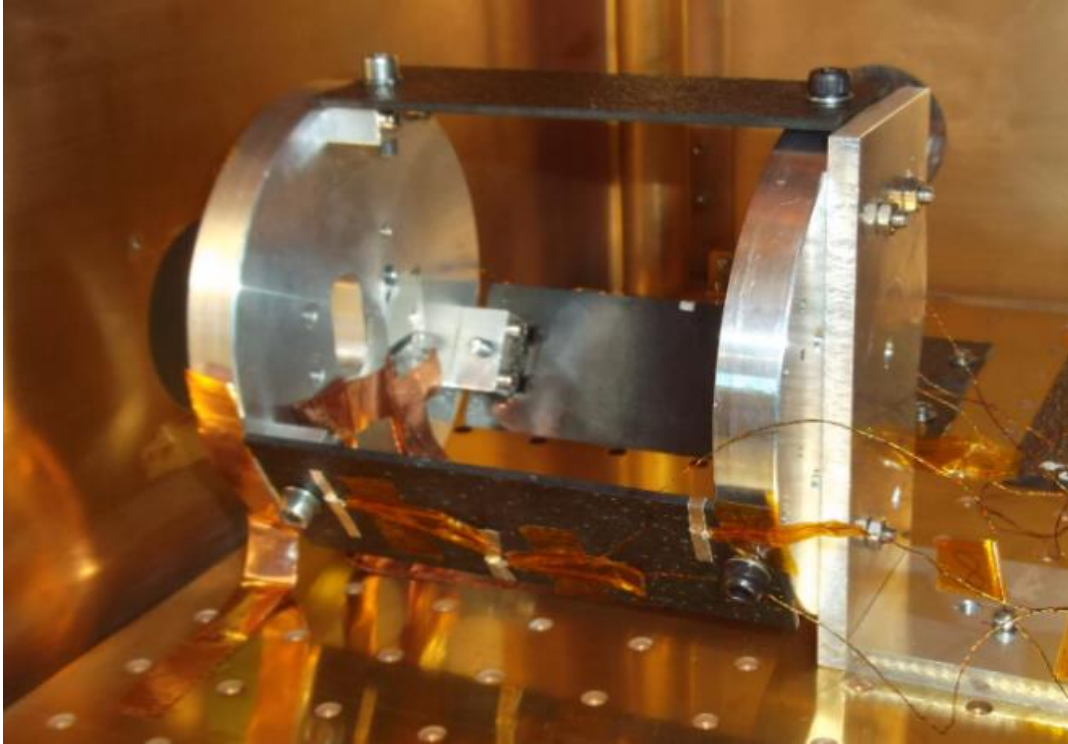


Figure 9. The tripod system with CFRP plate samples installed. The system was positioned horizontally inside the TFC with the interferometer beams entering from a side viewport. Cernox™ RTDs are located at three positions on the CFRP plate, measuring the temperature gradient.

4.2 Results

The thermal expansion of CFRP was measured down to an average sample temperature of 20 K. Lower temperatures were not reached due to the high emissivity of CFRP plates, as well as the low thermal conductivity of the samples, leading to large thermal gradients across the samples induced by stray light through the viewports in the 4 K chamber. Two sets each of three different types of samples were measured. The samples were distinguished by the orientation of carbon fibers. One set had fibers oriented along the measurement axis (called the 0° axis), another sample set had fibers oriented perpendicular to the measurement axis (90° axis), and the last sample set had layers of alternating orientations stacked together in a “quasi-isotropic” configuration.

As shown in Figure 10, thermal contraction was minimal along the axis of the fibers and at a maximum when perpendicular to fiber orientation. This follows from theoretical expectations, because the thermal contraction of the epoxy matrix is much greater than that of the carbon fibers. The thermal contraction of the quasi-isotropic sample fell between these extreme cases. With this technique of measuring thermal contraction, a measurement precision of 10 nm was achieved, proving that this technique is viable for the measurement of small dimensional changes in low thermal expansion materials at cryogenic temperatures. While initially we were concerned that the vibrations induced by the PTC would preclude precision metrology measurements during the cool down phase of the TFC, the differential nature of the measurement and the mechanical isolation provided by the copper braids have allowed such measurements.

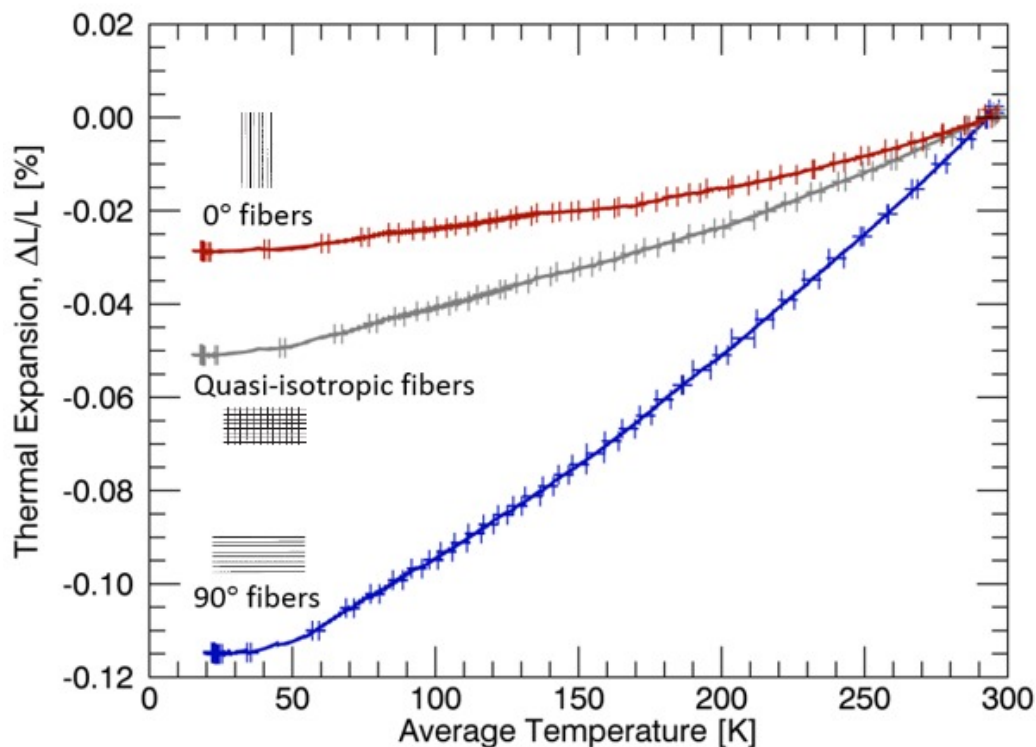


Figure 10. Thermal expansion results of the CFRP plates from room temperature to 20 K. Error bars shown are shown ever 50 data points and represent 1σ uncertainties. The temperature uncertainty was the dominant source of error, due to the thermal gradient present along the CFRP plates while cooling.

5. FUTURE WORK

5.1 Second PTC

With the addition of the second pulse tube cooler working in parallel with the currently installed unit, there will be a dramatic increase in the performance of the cryostat. The cooling time is expected to be cut in half with a significant part of the 1.5 W cooling power of the second PTC available at 4 K.

5.2 Cryogenic Iris

The use of external instrumentation requires a window in the TFC. In the current configuration a single pulse tube cooler is not sufficient to cool the system to 4 K with a window open to the laboratory environment. The total radiant power through a window (40 mm diameter), calculated by the Stefan-Boltzmann Law amounts to:

$$P_{rad} = A\sigma T^4 \approx 0.5 W \quad (2)$$

Where A is the diameter of the window, T is 295 K, and σ is the Stefan-Boltzmann constant. This heat input is double the residual cooling power of the TFC at 4.2 K, increasing the base temperature of the TFC to 5 K. To address this concern a cryogenic, motorized, zero aperture iris has been designed and developed which will allow the TFC to reach a base temperature of 4 K with the iris closed.

5.3 Thermal Braids

The copper braids which serve to decouple mechanical vibrations of the pulse tube from the cold plate also limit the cooling power supplied to the cold plates. In Figure 8, the thermal gradient which is present between the 45 K cold head and the 45 K plate is evidence of this. Thermal calculations show that the actual cooling power supplied to the 45 K plate is 13 W, rather than the intended 40 W. By modifying the braids (i.e. decreasing the length or increasing the cross-sectional area), there will be more available cooling power at the 45 K plate. The result of this modification will be a decreased temperature of the 45 K shields, which should result in an increase in available cooling power at the 4 K stage.

5.4 Mechanical Feedthroughs

Mechanical feedthroughs have not yet been incorporated into the design, but will be added to enable application of external loads to internal components in order to measure mechanical properties of materials at low temperatures (e.g. Young's modulus).

5.5 Computer Controlled

All of the ancillary equipment associated with the TFC (vacuum pump, pulse tube compressor, Resistance Bridge, differential laser interferometer, autocollimator etc.) have the capability of being controlled remotely. Our goal is to fully automate and remotely control of the facility.

6. ACKNOWLEDGEMENTS

The AIG would like to acknowledge Quantum Technology Corporation for their contribution to the development of the TFC, in particular Yan Pennec and Steve Marshall for their assistance in the assembly and initial testing of the TFC. The authors also acknowledge support from the Canada Foundation for Innovation, the Canadian Space Agency, EU FP7-FISICA, and NSERC.

7. REFERENCES

- [1] Pilbratt, G. L., et al. "Herschel Space Observatory-An ESA facility for far-infrared and submillimetre astronomy," *Astronomy & Astrophysics* 518 (2010): L1.
- [2] Nakagawa, Takao, Hideo Matsuhara, and Yasuhiro Kawakatsu. "The next-generation infrared space telescope SPICA." *Proc. SPIE* 8442, 84420O, (2012).
- [3] Naylor, David A., et al. "In-orbit performance of the Herschel/SPIRE imaging Fourier transform spectrometer: lessons learned." *Proc. SPIE* 9143, 91432D (2014).
- [4] Jones, Martyn, et al. "CFRP mirror technology for cryogenic space interferometry: review and progress to date." *Proc. SPIE* 9904, 9904-237, (2016).
- [5] Veenendaal, Ian T., Naylor, David A., and Gom. Brad G. "Design of a cryogenic test facility for evaluating the performance of interferometric components of the SPICA/SAFARI instrument," *Proc. SPIE* 9143, 914345 (2014).
- [6] <http://www.cryomech.com/products/cryorefrigerators/pulse-tube/pt415/>
- [7] <http://cryogenics.nist.gov/MPropsMAY/materialproperties.htm>
- [8] http://www.detoronics.com/products/DT_MIL-DTL-26482_Series_I.html
- [9] <http://www.lakeshore.com/products/cryogenic-accessories/wire/pages/Overview.aspx>
- [10] <http://www.renishaw.com/en/rld10-differential-interferometer--6492>
- [11] <http://www.plxinc.com/products/all-in-one-electronic-autocollimator-and-alignment-telescope>
- [12] <https://shop.edwardsvacuum.com/products/a73001983/view.aspx>
- [13] <http://www.mksinst.com/product/product.aspx?ProductID=445>